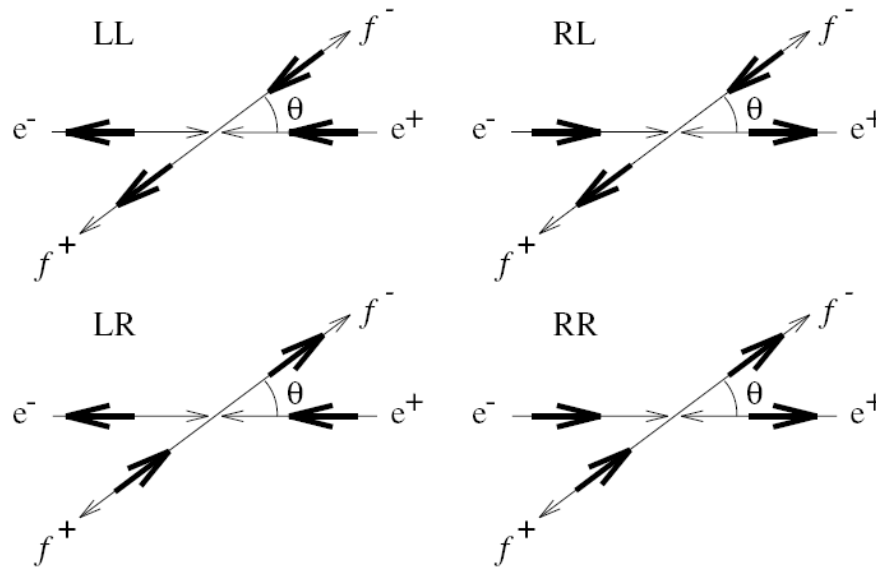


Instead of measuring the spin averaged transition amplitudes try to decompose the different “helicity” components to the cross section:



Observables:

$$\sigma_{LL} + \sigma_{RR}$$

$$\sigma_{RL} + \sigma_{LR}$$

Related to σ_F and σ_B .

$$\sigma_L = \sigma_{LL} + \sigma_{LR}$$

$$\sigma_R = \sigma_{RL} + \sigma_{RR}$$

$$\sigma_- = \sigma_{LL} + \sigma_{RL}$$

$$\sigma_+ = \sigma_{RR} + \sigma_{LR}$$

$$A_{FB} = \frac{\sigma_F - \sigma_B}{\sigma_F + \sigma_B}$$

Forward-backward asym.

$$A_{LR} = \frac{\sigma_L - \sigma_R}{\sigma_L + \sigma_R}$$

Left right asym. (initial)

$$\mathcal{P}_f = \frac{\sigma_+ - \sigma_-}{\sigma_+ + \sigma_-}$$

fermion polarization (final)

Forward-backward asymmetry

Angular distribution: (see above)

$$F_{\gamma Z}(\cos \theta) = \frac{Q_e Q_\mu}{4 \sin^2 \theta_W \cos^2 \theta_W} \left[2g_V^e g_V^\mu (1 + \cos^2 \theta) + 4g_A^e g_A^\mu \cos \theta \right]$$

$$F_Z(\cos \theta) = \frac{1}{16 \sin^4 \theta_W \cos^4 \theta_W} \left[(g_V^{e^2} + g_A^{e^2})(g_V^{\mu^2} + g_A^{\mu^2})(1 + \cos^2 \theta) + 8g_V^e g_A^e g_V^\mu g_A^\mu \cos \theta \right]$$

Very small: $g_V \approx 0$

Forward-backward asymmetry A_{FB} $\frac{d\sigma}{d \cos \theta} \sim (1 + \cos^2 \theta) + \frac{8}{3} A_{FB} \cos \theta$

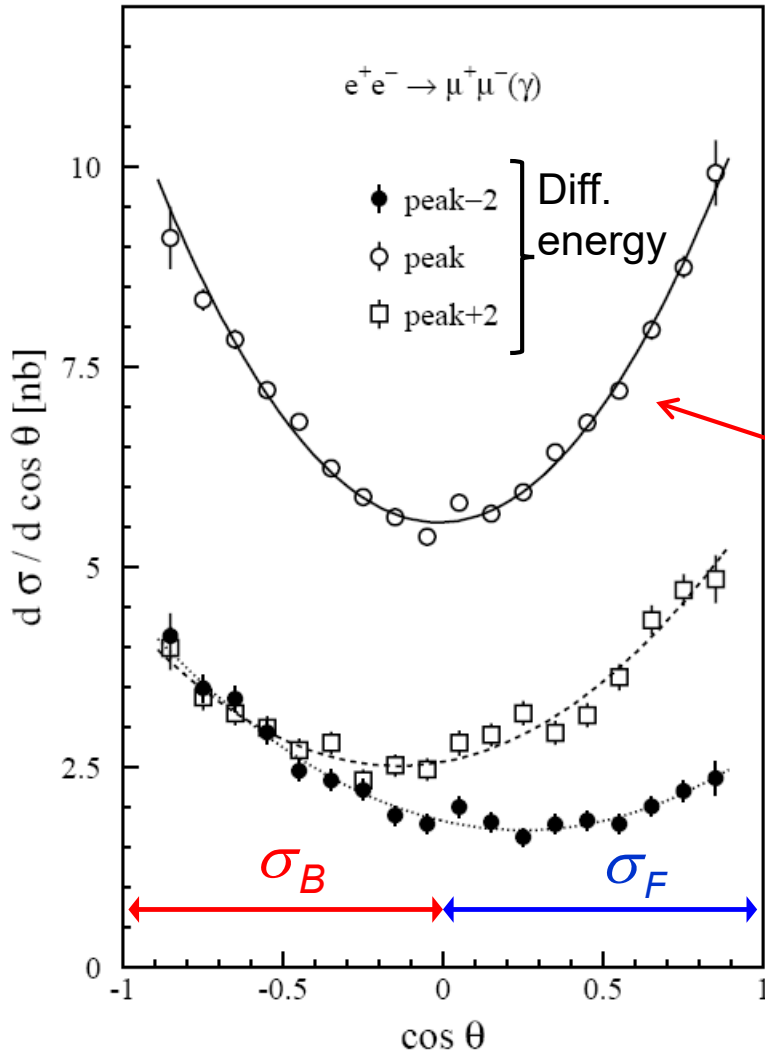
- Away from the resonance large \rightarrow interference term dominates

$$A_{FB} \sim g_A^e g_A^f \cdot \frac{s(s - M_Z^2)}{(s - M_Z^2)^2 + M_Z^2 \Gamma_Z^2} \rightarrow \text{large}$$

- At the Z pole: Interference = 0 (see energy dependence of interference term)

$$A_{FB} = 3 \cdot \frac{g_V^e g_A^e}{(g_V^e)^2 + (g_A^e)^2} \cdot \frac{g_V^\mu g_A^\mu}{(g_V^\mu)^2 + (g_A^\mu)^2}$$

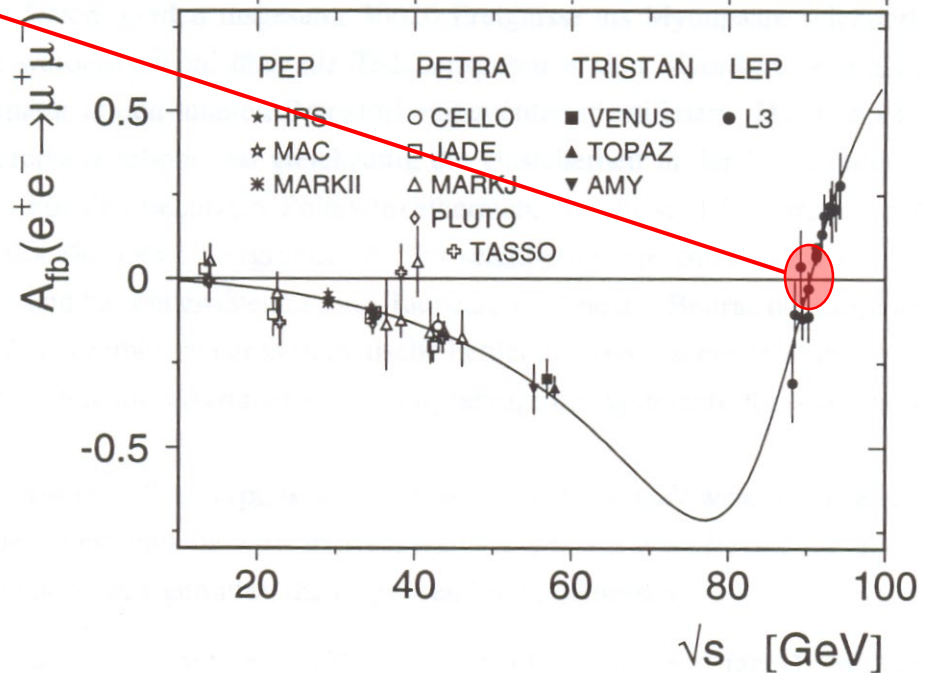
\rightarrow very small because g_V^l small in SM



$$\frac{d\sigma}{d\cos\theta} \sim (1 + \cos^2\theta) + \frac{8}{3} A_{FB} \cos\theta$$

with $A_{FB} = \frac{\sigma_F - \sigma_B}{\sigma_F + \sigma_B}$

$$\sigma_{F(B)} = \int_{0(-1)}^{1(0)} \frac{d\sigma}{d\cos\theta} d\cos\theta$$



Determination of the couplings g_A and g_V

Asymmetrie at the Z pole

$$A_{FB} \sim g_A^e g_V^e g_A^f g_V^f$$

Cross section at the Z pole

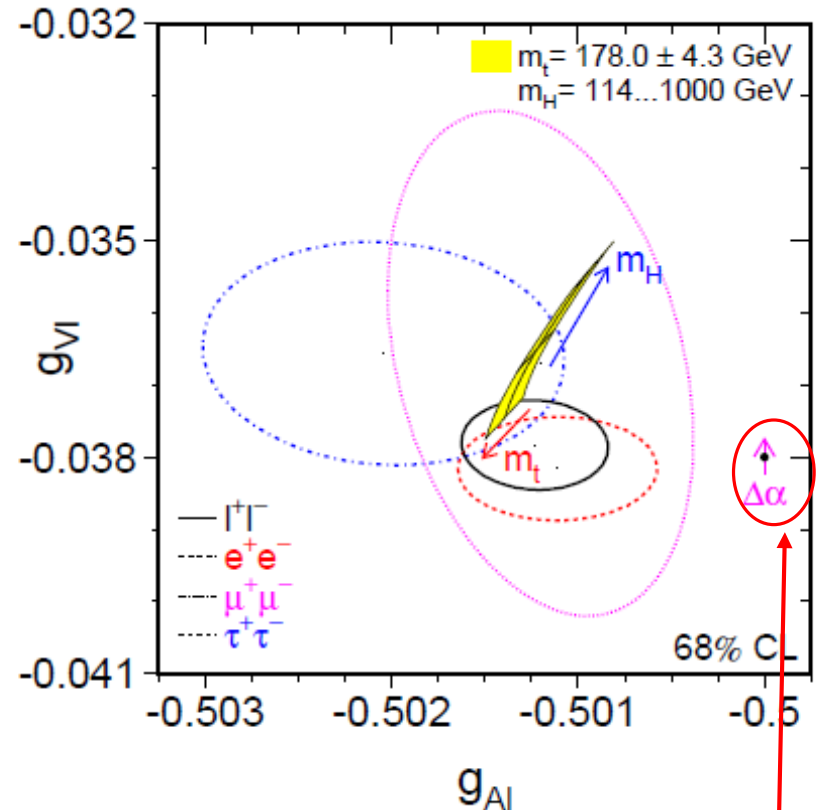
$$\sigma_Z \sim \left[(g_V^e)^2 + (g_A^e)^2 \right] \left[(g_V^f)^2 + (g_A^f)^2 \right]$$



Lepton asymmetries together with lepton pair cross sections allow the determination of the lepton couplings g_A and g_V . → **elliptical confidence regions**

Good agreement between the 3 lepton species confirms “lepton universality”

Different contour size: electrons are measured in all measurements; tau contour uses additional measurement (polarization)



Lowest order SM prediction

Deviation from lowest order SM prediction
 $g_V = T_3 - 2q \sin^2 \theta_W$ $g_A = T_3$ $\sin^2 \theta_W = 1 - \frac{m_W^2}{m_Z^2}$
 is an effect of higher-order loop-corrections

Assuming lepton universality:

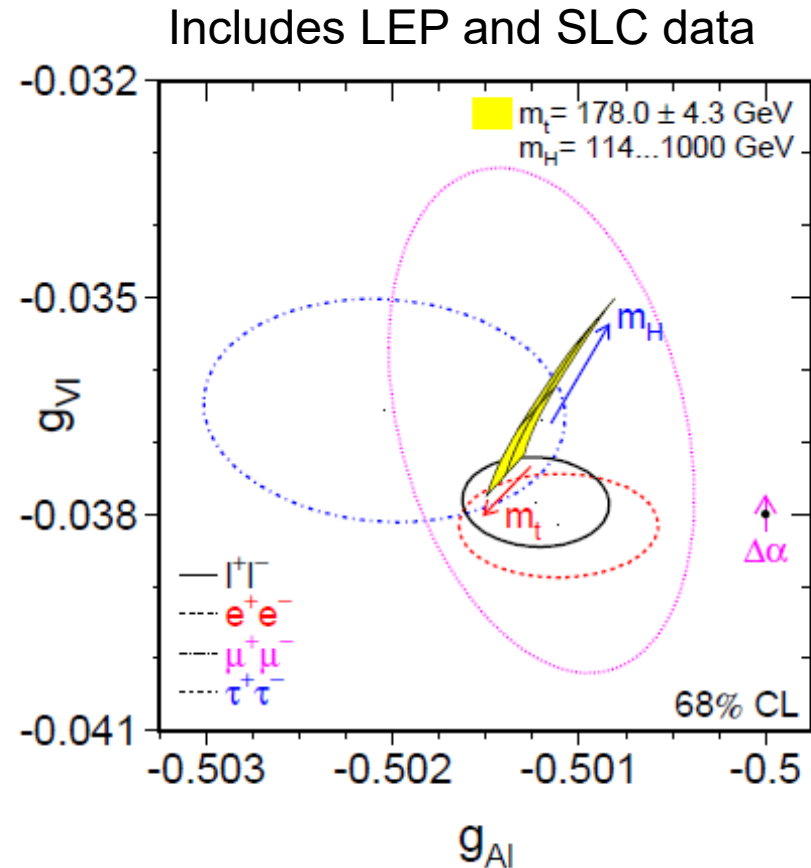
$$g_V^\ell = -0.03783 \pm 0.00041$$

$$g_A^\ell = -0.50123 \pm 0.00026$$

$$g_R^\ell = +0.23170 \pm 0.00025$$

$$g_L^\ell = -0.26959 \pm 0.00024$$

Z boson couples stronger to LH leptons than to RH leptons.



From g_V one can calculate $\sin^2\theta_w$

$$g_V^f = I_3^f - 2Q_f \sin^2 \theta_w \quad \longrightarrow \quad \sin^2 \theta_w^{\text{eff}} = 0.23113 \pm 0.00021$$

Left-Right Asymmetry at Stanford Linear Collider (SLC)

Measure cross section σ_L (σ_R) for LH (RH) polarized initial electrons:
Longitudinal polarization possible difficult at a circular collider.

$$A_{LR} = \frac{1}{\mathcal{P}_e} \frac{\sigma_L^f - \sigma_R^f}{\sigma_L^f + \sigma_R^f}$$

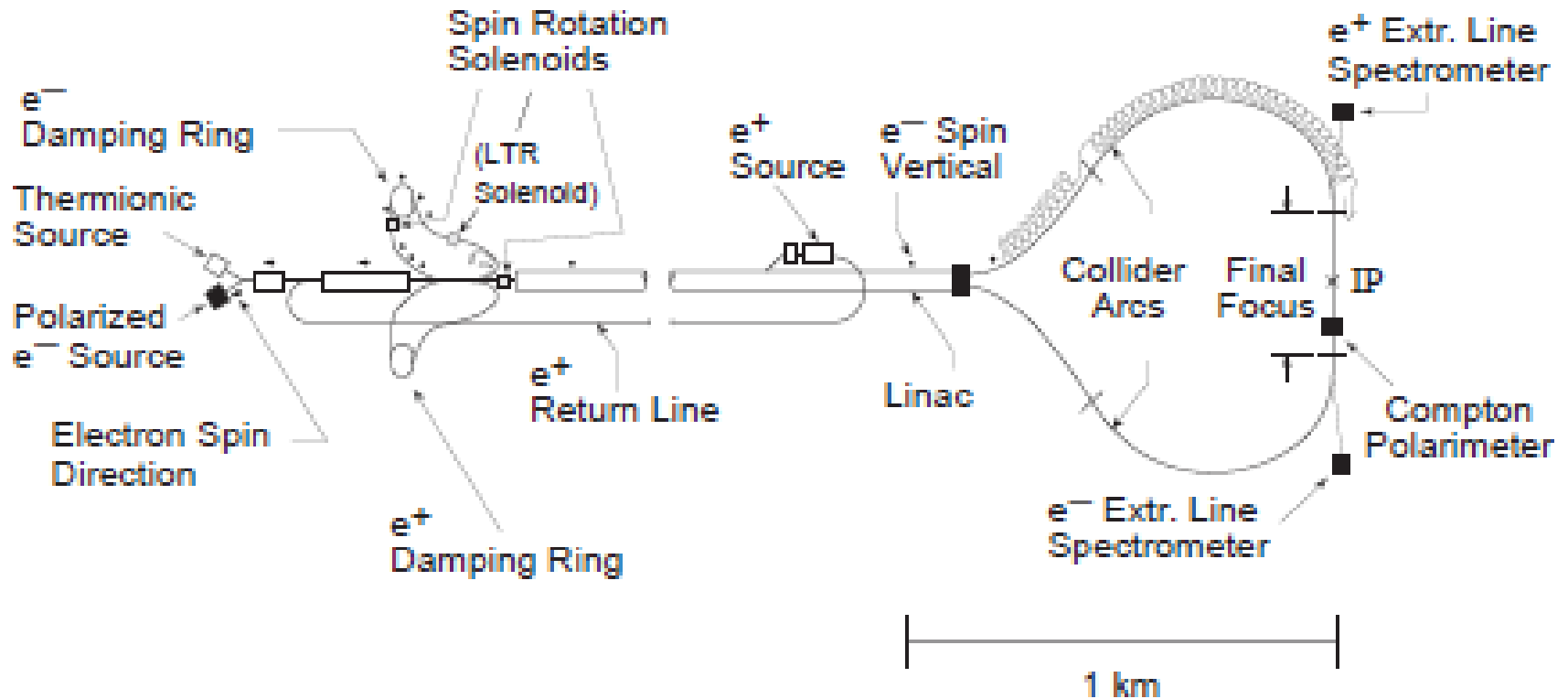
Polarization of electron beam \mathcal{P}_e :
 $\mathcal{P}_e \sim 70 - 80\%$

$$A_{LR} = \frac{2g_V^e g_A^e}{(g_V^e)^2 + (g_A^e)^2} = \frac{2(1 - 4 \sin^2 \theta_w)}{1 + (1 - 4 \sin^2 \theta_w)^2}$$

Powerful determination of $\sin^2 \theta_w$.

Requires longitudinal polarization of colliding beams

SLAC Linear Collider



- Longitudinal polarized electrons from polarized laser light (photo effect)
- Spin rotation to produce transverse polarized electrons
- Spin again rotated in the final arcs – longitudinal orientation (70-80%)

Precise determination of beam polarization using a Compton Polarimeter

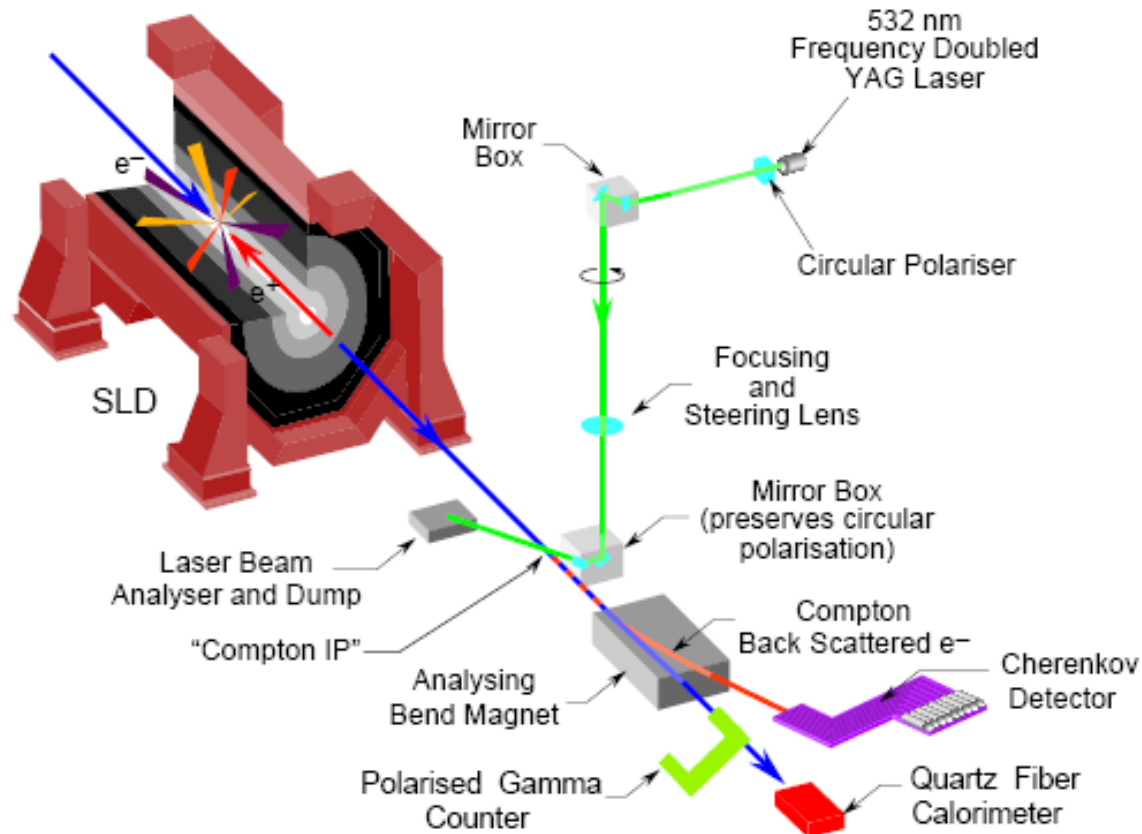
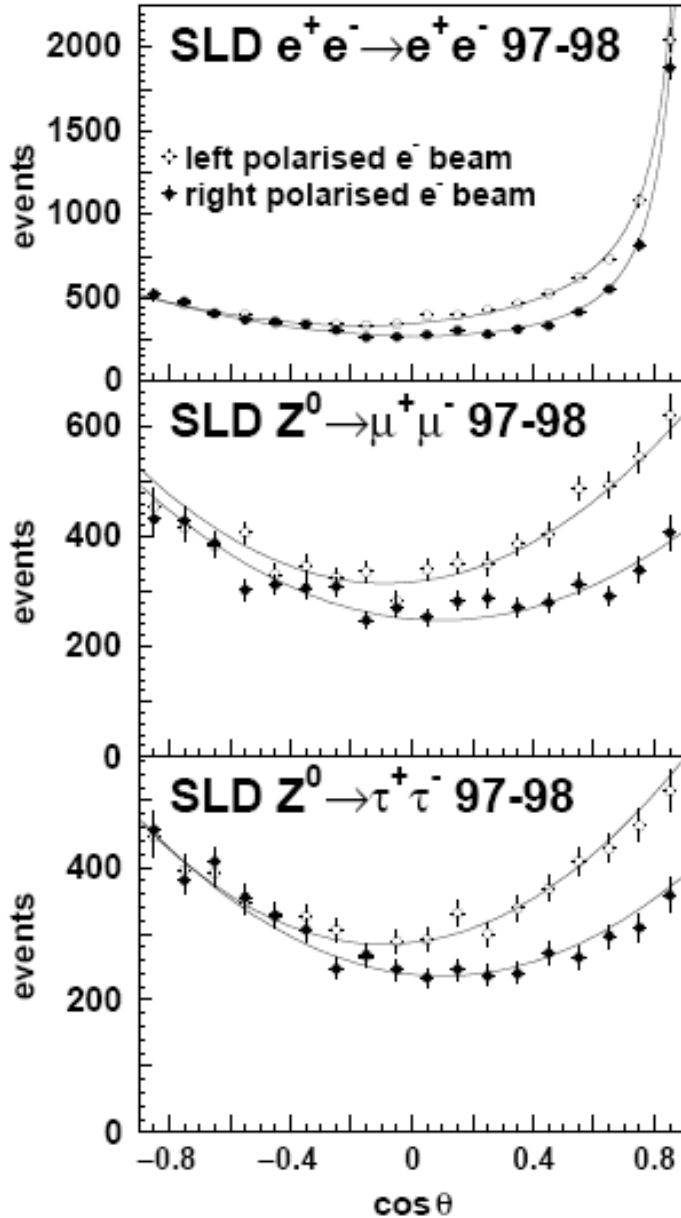


Figure 3.1: A conceptual diagram of the SLD Compton Polarimeter. The laser beam, consisting of 532 nm wavelength 8 ns pulses produced at 17 Hz and a peak power of typically 25 MW, were circularly polarised and transported into collision with the electron beam at a crossing angle of 10 mrad approximately 30 meters from the IP. Following the laser/electron-beam collision, the electrons and Compton-scattered photons, which are strongly boosted along the electron beam direction, continue downstream until analysing bend magnets deflect the Compton-scattered electrons into a transversely-segmented Cherenkov detector. The photons continue undeflected and are detected by a gamma counter (PGC) and a calorimeter (QFC) which are used to cross-check the polarimeter calibration.

LR asymmetries for leptonic final states :



SLD

Asymmetry
clearly seen for
LH and RH
cross section.

SLD

All data:

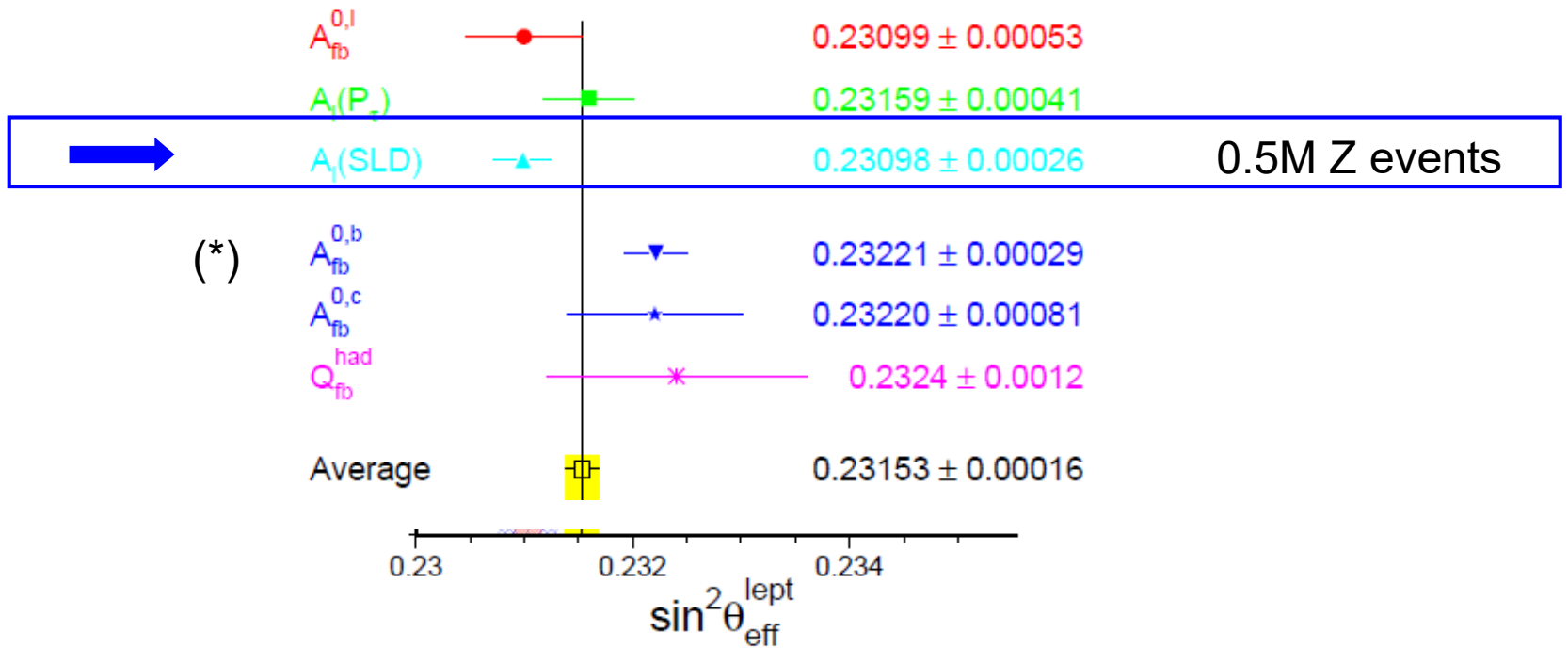
$$A_{LR} = 0.1513 \pm 0.0021$$

$$\sin^2 \theta_w = 0.23098 \pm 0.00026$$

$$A_{LR} = \frac{2(1 - 4\sin^2 \theta_w)}{1 + (1 - 4\sin^2 \theta_w)^2}$$

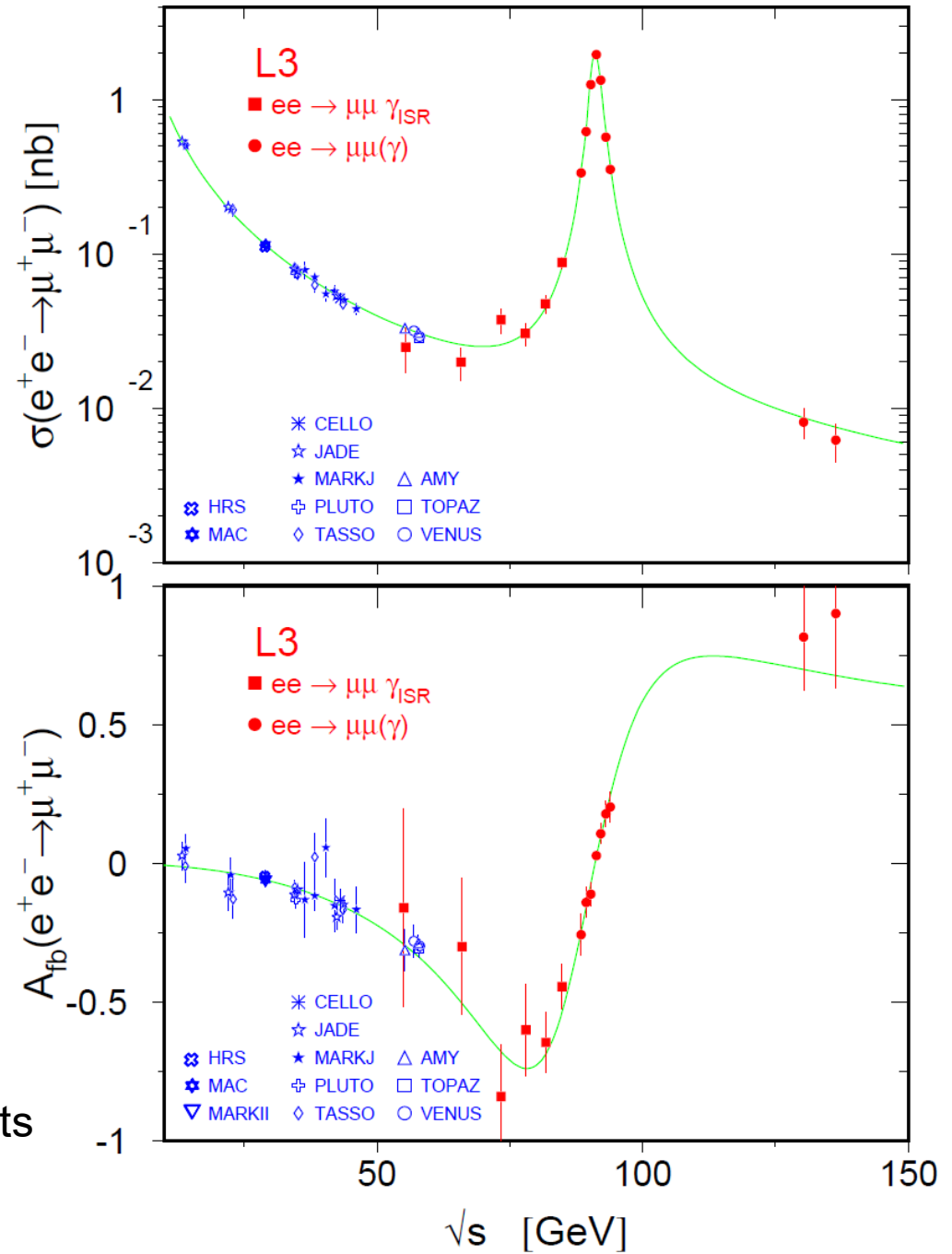
With 0.5×10^6
Z-decays

SLD versus $4 \times 4.5 \times 10^6$ Z-decays at LEP



(*) One can also determine the forward-backward asymmetry for bb and cc-events.

$$e^+e^- \rightarrow \mu^+\mu^-(\gamma)$$



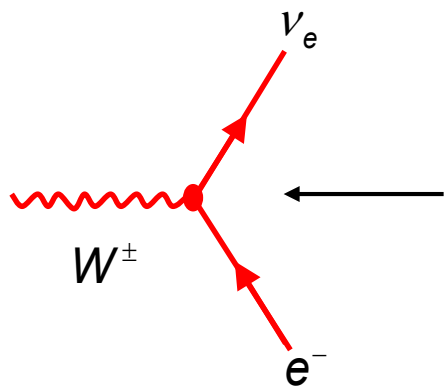
... I am still a bit proud of these plots

2. Precision test of the W sector (LEP2, Tevatron, LHC)

Plots and results – if not mentioned differently – take from:

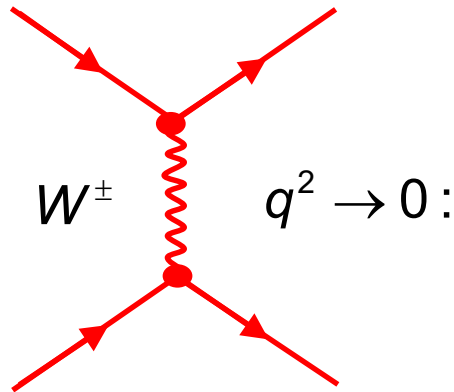
ALEPH, DELPHI, L3 and OPAL Collaborations,
Electroweak measurements in electron–positron collisions at
W-boson-pair energies at LEP,
<https://doi.org/10.1016/j.physrep.2013.07.004>

Recap: W couplings

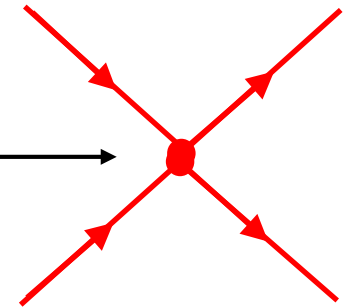


Vertex factors

$$-i \frac{g}{\sqrt{2}} \gamma_\mu \frac{1}{2} (1 - \gamma^5)$$



$$\frac{g^2}{8M_W^2} = \frac{G_F}{\sqrt{2}}$$



W branching fractions

(lowest order, no QCD corrections, $N_C = 3$)

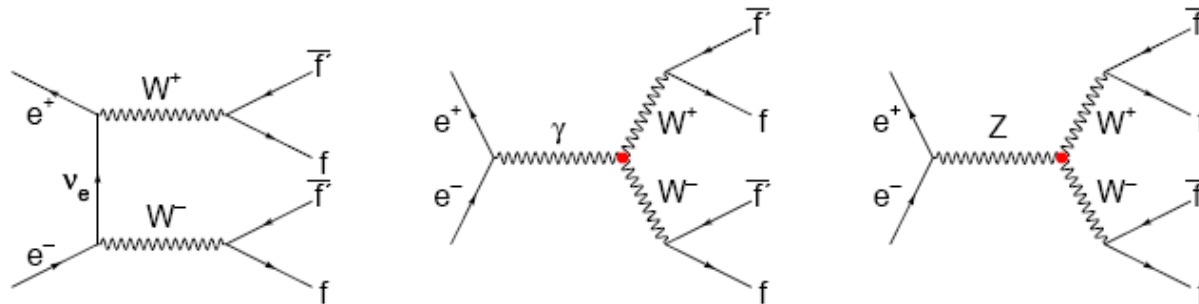
$$\Gamma_{e\nu} = \Gamma_{\mu\nu} = \Gamma_{\tau\nu} \approx 11.1\%$$

$$\Gamma_{qq} \approx 66.6\%$$

W-pair production at LEP2 ($\sqrt{s} > 161$ GeV)

At LEP: $e^+e^- \rightarrow WW \rightarrow f\bar{f}f\bar{f}$

~ 10 K WW events / LEP-experiment



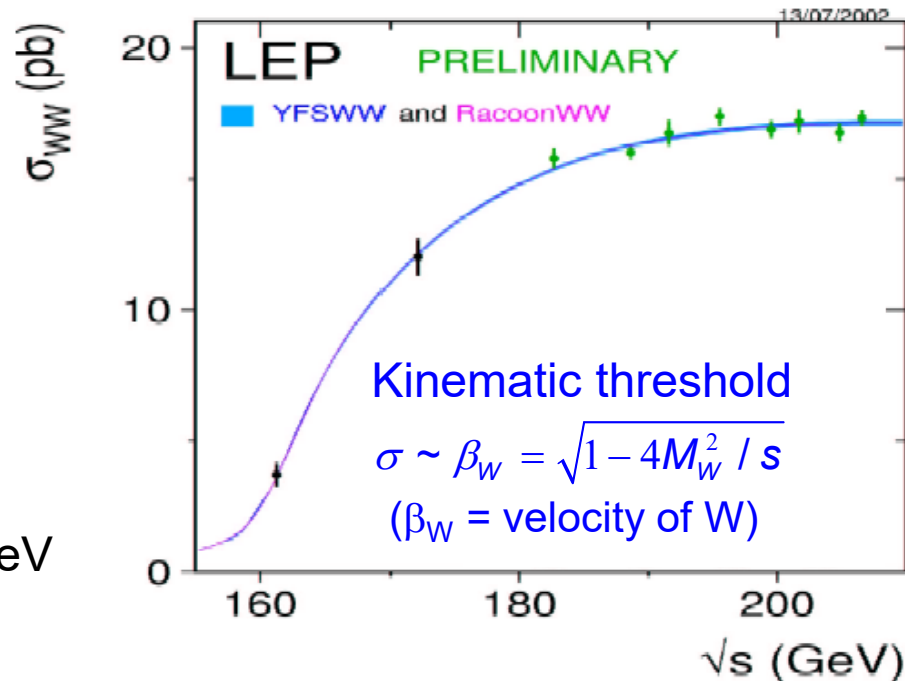
Threshold behavior of the cross section (kinematics, phase space) for $ee \rightarrow WW$ production:



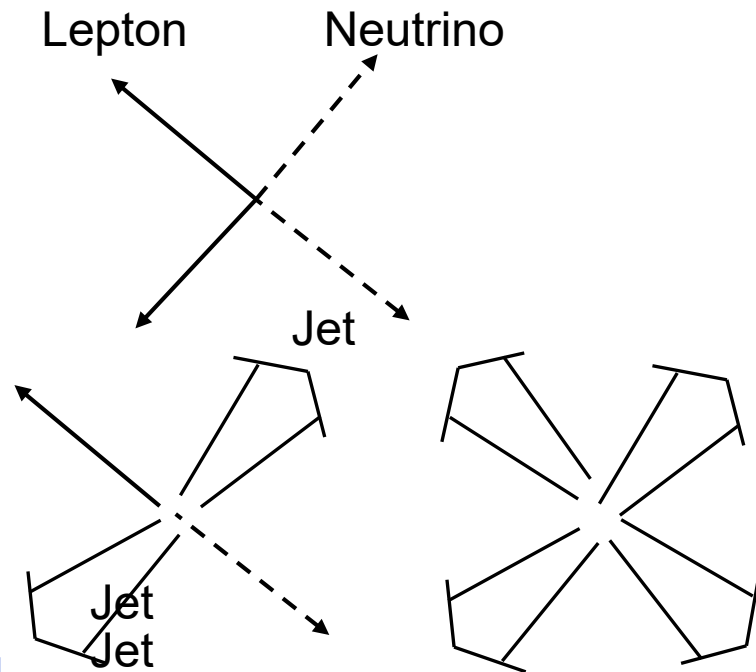
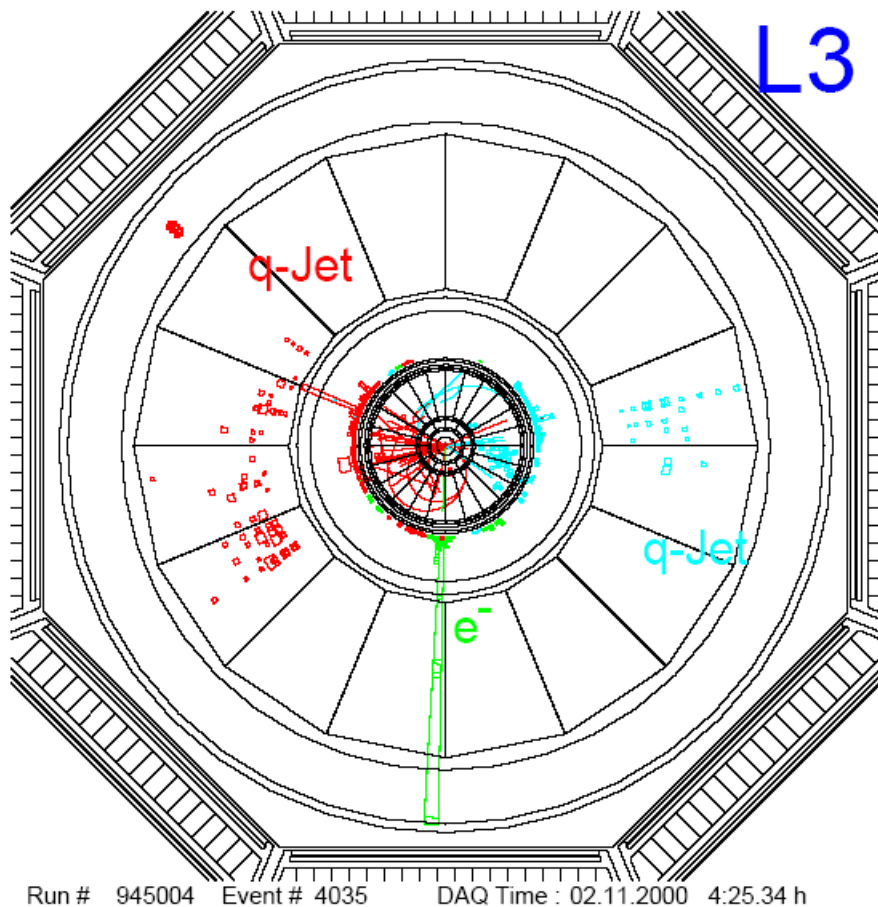
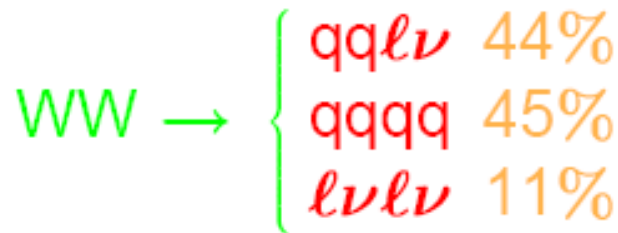
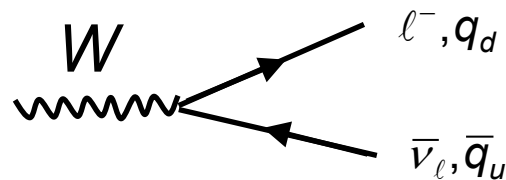
Phase space factor = $f(M_W, \sqrt{s})$:

→ Allows determination of M_W

$$m_W = 80.42 \pm 0.20 \pm 0.03(E_{\text{LEP}}) \text{ GeV}$$



Topology of W decays

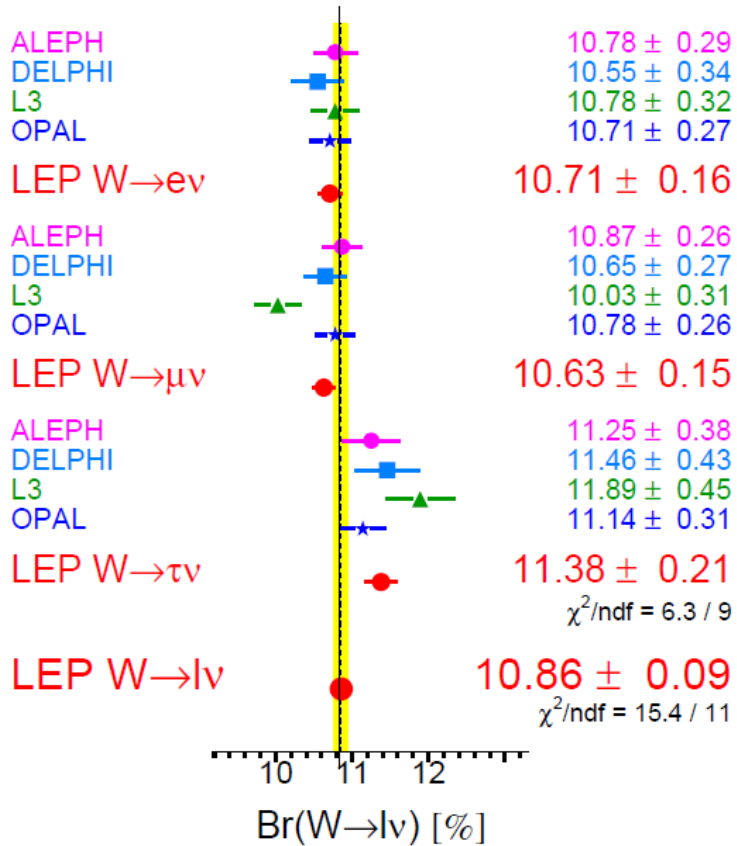


Signatures for a mass measurement:

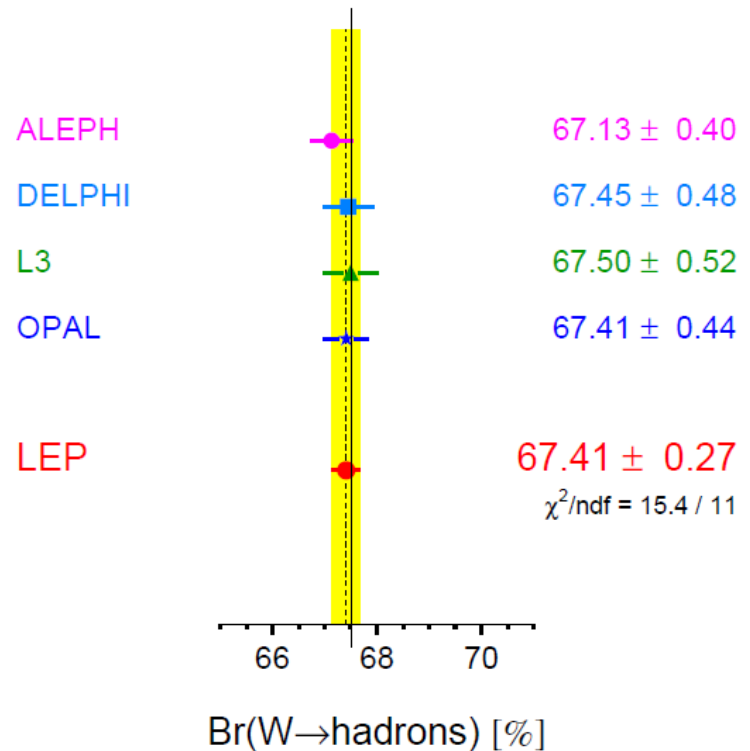
$W_1 \rightarrow l\nu$ $W_2 \rightarrow \text{JetJet}$ or $W_1 \rightarrow \text{JetJet}$ $W_2 \rightarrow \text{JetJet}$

Use dijet invariant mass.

W Leptonic Branching Ratios

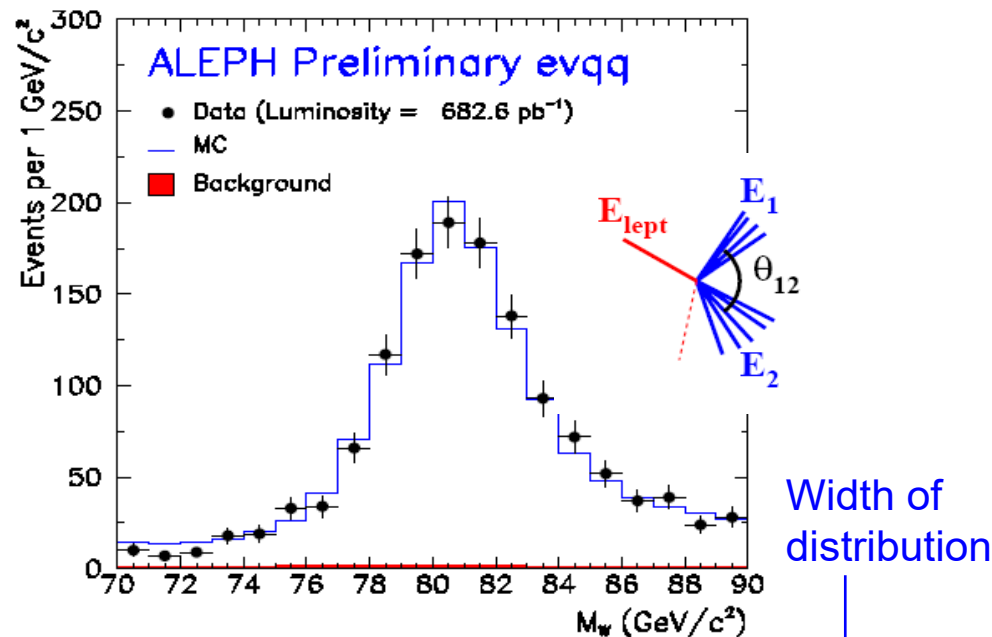
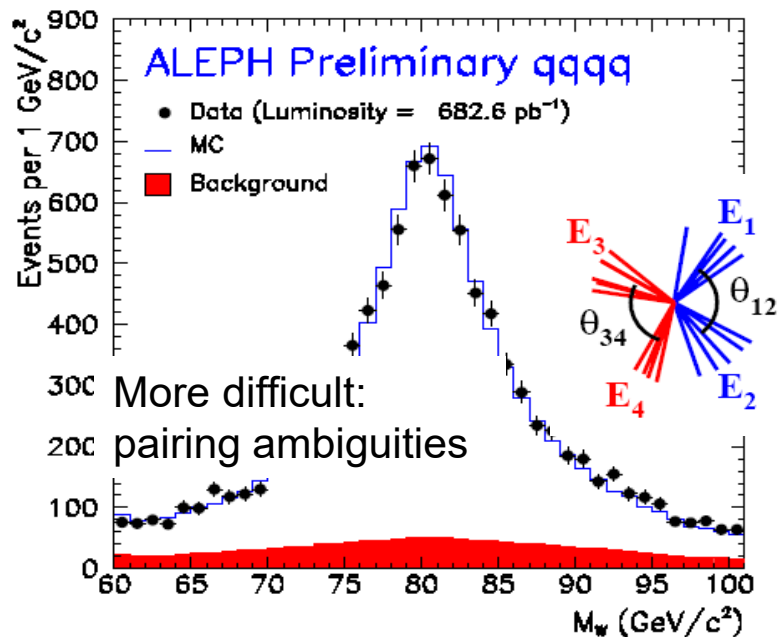


W Hadronic Branching Ratio

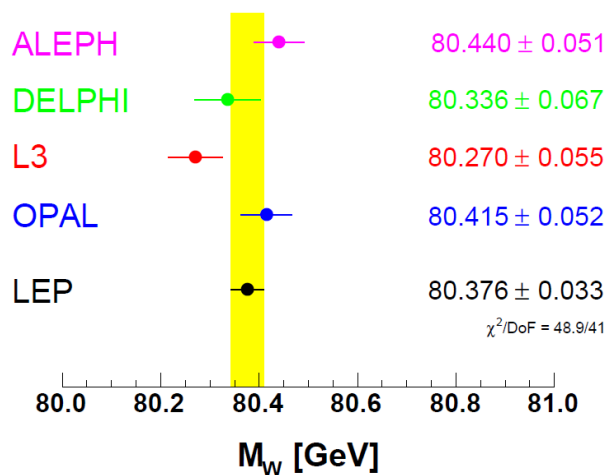


Agreement between leptons tests
lepton universality

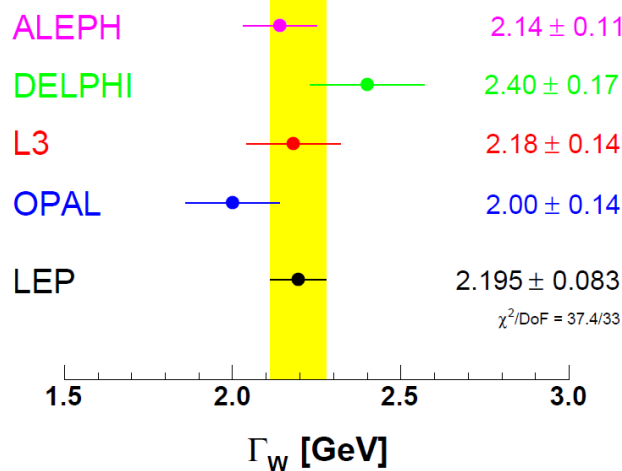
W mass and Γ_W reconstruction from dijet mass distr.



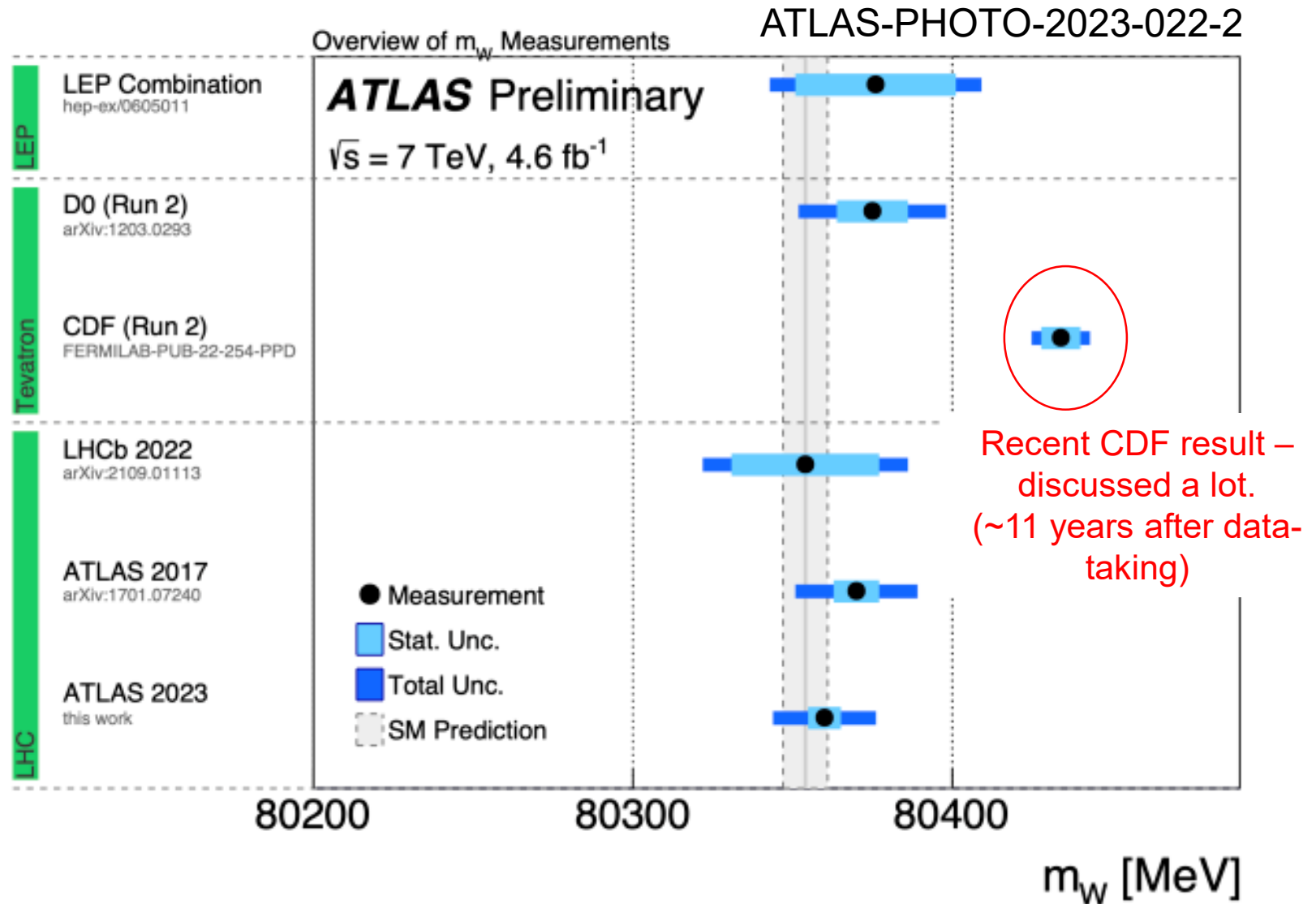
LEP W-Boson Mass



LEP W-Boson Width

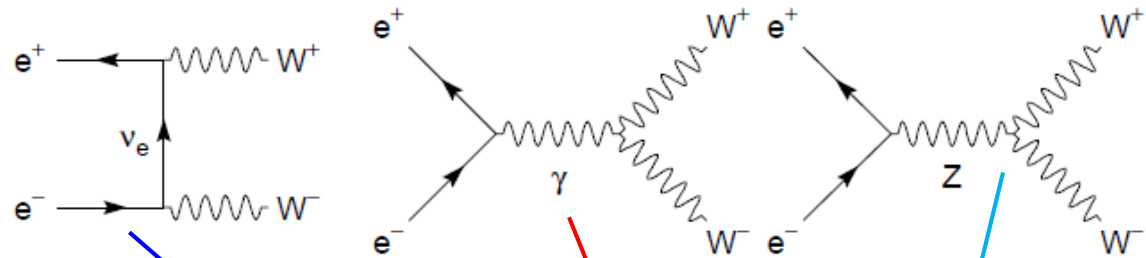


Dijet mass reconstruction also possible at Tevatron ($p\bar{p}$ @ 2 TeV) and LHC (pp @ 13 TeV)



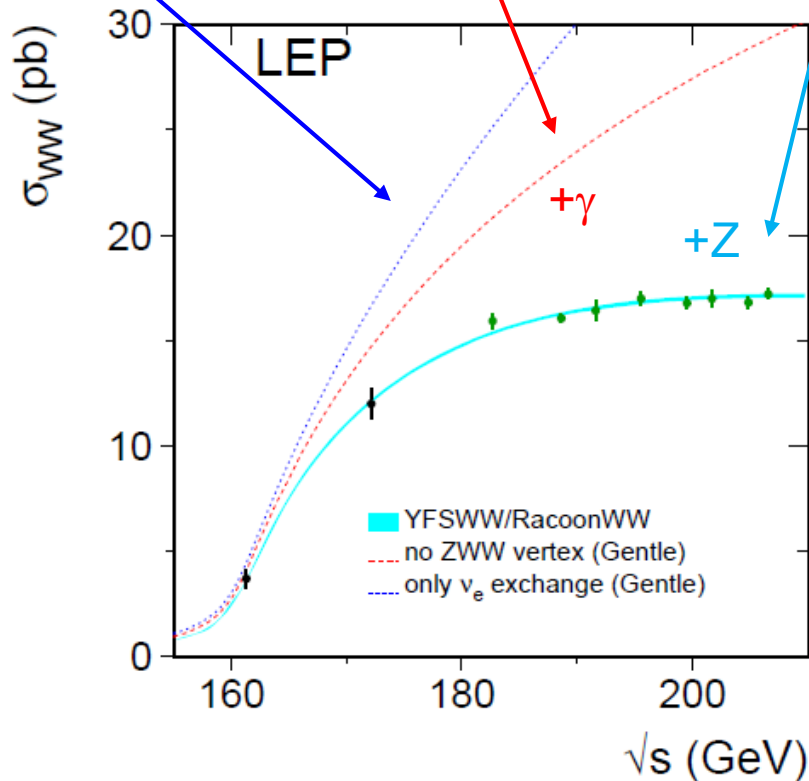
Triple Gauge Boson Coupling

$$e^+ e^- \rightarrow WW$$

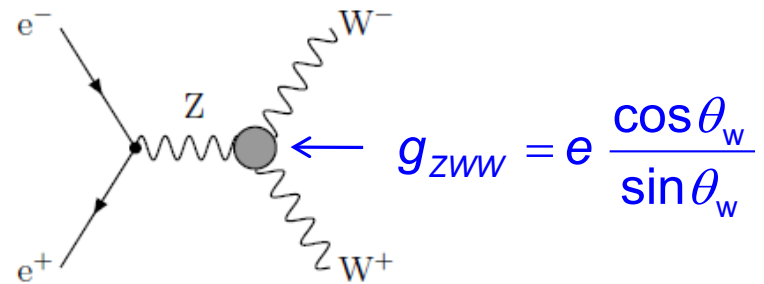
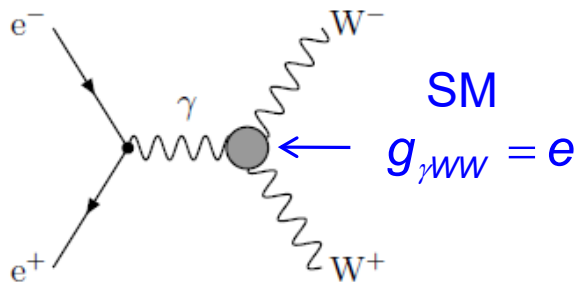


Cross section data confirms the existence of the γ/ZWW triple gauge boson vertex.

Can one test the coupling strength?



Test of trilinear gauge boson coupling in WW production



Triple gauge coupling an important result of the non-abelian gauge structure: we are interested in the strength and in the Lorentz structure of coupling.

Most general Lorentz invariant Lagrangian which describes the triple gauge boson interaction has fourteen independent complex couplings, seven describing the $WW\gamma$ vertex and seven describing the WWZ vertex.

Electromagnetic gauge invariance and C and P conservation reduced the number of independent TGCs to five. Common choice $\{g_Z^1, \kappa_\gamma, \kappa_Z, \lambda_\gamma, \lambda_Z\}$.

Standard Model: $g_Z^1 = \kappa_\gamma = \kappa_Z = 1$

$$\lambda_\gamma = \lambda_Z = 0$$

$$\kappa_Z = g_1^Z - (\kappa_\gamma - 1) \tan^2 \theta_W,$$

$$\lambda_Z = \lambda_\gamma,$$

Additional constraints

Interpretation of γWW couplings:

$$\mu_W = \frac{e}{2m_W} (1 + \kappa_\gamma + \lambda_\gamma),$$

$$q_W = -\frac{e}{m_W^2} (\kappa_\gamma - \lambda_\gamma).$$

magnetic dipole moment
quadrupole moment

Measurements requires an angular analysis of the W bosons as well as of the final state particles: 5 angles (vector Ω) = W^- production polar angle, the polar and azimuthal angles, of the decay fermions from the W^- and the W^+ in the W rest frame (sound complicated but this type of analysis is very common...).

See e.g. OPAL, CERN-EP/2000-114

Fit angular distribution to the differential cross section:

$$d\sigma(\Omega, \alpha) = S^{(0)}(\Omega) + \sum_i \alpha_i \cdot S_i^{(1)}(\Omega) + \sum_{i,j} \alpha_i \alpha_j \cdot S_{ij}^{(2)}(\Omega), \quad \alpha_i = \Delta\kappa_\gamma, \Delta g_1^Z \text{ and } \lambda,$$

Average of 4 LEP experiments

Parameter	68% C.L.	95% C.L.	SM
g_1^Z	$+0.984^{+0.018}_{-0.020}$	[0.946, 1.021]	1
κ_γ	$+0.982^{+0.042}_{-0.042}$	[0.901, 1.066]	1
λ_γ	$-0.022^{+0.019}_{-0.019}$	[-0.059, 0.017]	0

CERN-PH-EP/2013-022

arXiv:1302.3415

3. Higher order loop corrections

Recap: “Tree-level” Standard Model relations

Fermi constant:

$$G_F = \frac{\pi\alpha}{\sqrt{2}m_W^2 \sin^2 \theta_W^{\text{tree}}}, \quad \leftarrow \text{Underlines tree-level}$$

Mixing angle and masses:

$$\rho_0 = \frac{m_W^2}{m_Z^2 \cos^2 \theta_W^{\text{tree}}} = 1$$

ρ -parameter is determined by the Higgs sector:
For a single Higgs-doublet (SM) $\rho_0 = 1$

ρ -parameter is also a measure of the strength of CC and NC interactions.

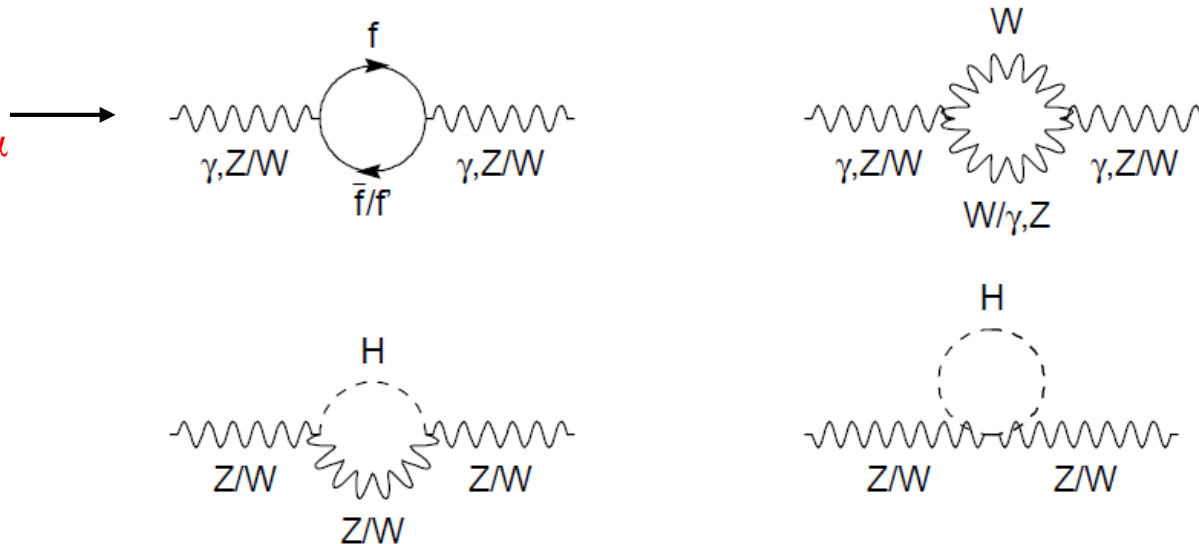
Z-couplings:

$$\begin{aligned} g_V^{\text{tree}} &\equiv g_L^{\text{tree}} + g_R^{\text{tree}} = \sqrt{\rho_0} (T_3^f - 2Q_f \sin^2 \theta_W^{\text{tree}}) \\ g_A^{\text{tree}} &\equiv g_L^{\text{tree}} - g_R^{\text{tree}} = \sqrt{\rho_0} T_3^f. \end{aligned}$$

$\uparrow = 1$ (SM, single H-doublet)

Higher order corrections to boson propagators:

In QED:
Running α



When these corrections are renormalized in the “on-shell” scheme the form of the equation for masses and mixing angle is maintained, and taken to define the on-shell electroweak mixing angle, θ_w , to all orders, in terms of the vector boson pole masses:

$$\frac{m_W^2}{m_Z^2 \cos^2 \theta_W} = 1$$

“on-shell” scheme: renormalized masses = pole masses (observed).

However, the relations between couplings and mixing angle change. This leads to the introduction of an effective mixing angle $\theta_{w,eff}$.

Considering high-orders one finds:

$$\Rightarrow \bar{\rho} = 1 + \Delta\rho$$

$$\Rightarrow \sin^2 \theta_{\text{eff}} = (1 + \Delta\kappa) \sin^2 \theta_W$$

$$g_{Vf} \equiv \sqrt{\rho_f} (T_3^f - 2Q_f \sin^2 \theta_{\text{eff}}^f)$$

$$g_{Af} \equiv \sqrt{\rho_f} T_3^f,$$

$$\frac{g_{Vf}}{g_{Af}} = 1 - 4|Q_f| \sin^2 \theta_{\text{eff}}^f$$

Ratio of NC / CC interaction:

$\sin^2 \theta_W$ in expression for couplings

because if vertex corrections
 ρ becomes dependent of fermion.

Relation between M_W and G_F

Running of α_{QED}

$$\Rightarrow m_W^2 = \frac{\pi\alpha}{\sqrt{2} \sin^2 \theta_W G_F} (1 + \Delta r)$$

$$\Rightarrow \alpha(m_Z^2) = \frac{\alpha(0)}{1 - \Delta\alpha}$$

$$\text{with : } \Delta\alpha = \Delta\alpha_{\text{lept}} + \Delta\alpha_{\text{top}} + \Delta\alpha_{\text{had}}^{(5)}$$

$$\Delta\rho, \Delta\kappa, \Delta r = f(m_t^2, \log(m_H), \dots)$$

Explicit dependence of the radiative corrections on the top mass and Higgs mass allowed a determination of m_{top} and M_H before their discovery:

$$\text{e.g.: } \Delta r(m_t, M_H) = -\frac{3\alpha \cos^2 \theta_w}{16\pi \sin^4 \theta_w} \frac{m_t^2}{M_W^2} - \frac{11\alpha}{48\pi \sin^2 \theta_w} \ln \frac{M_H^2}{M_W^2} + \dots$$

Determination of $\sin^2\theta_{w,\text{eff}}$ and the ρ -parameter

arXiv:hep-ex/0509008

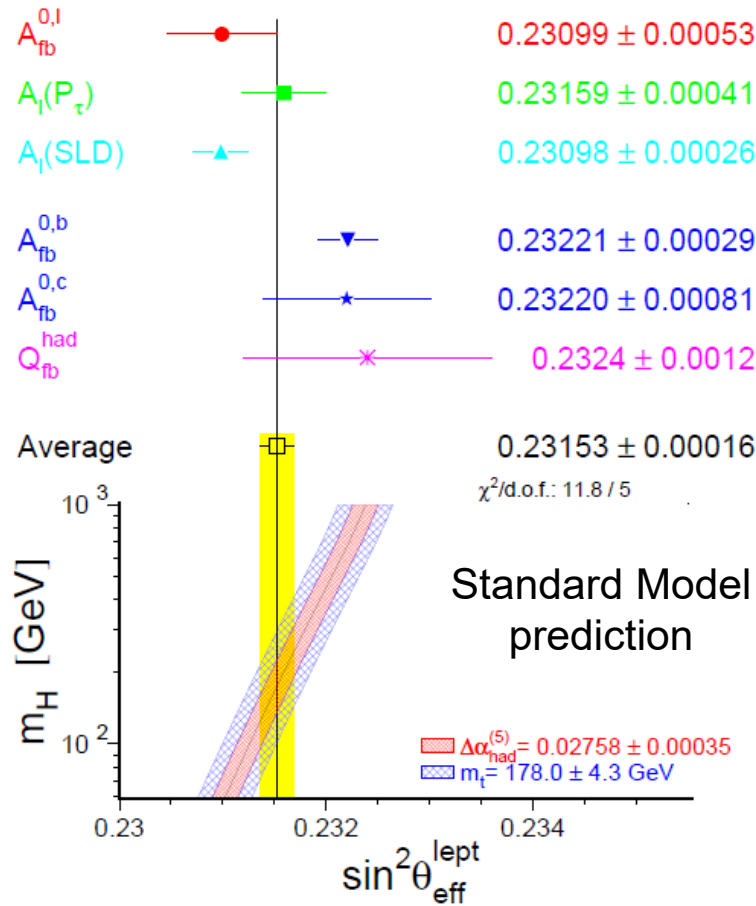


Figure 7.6: Comparison of the effective electroweak mixing angle $\sin^2\theta_{\text{eff}}^{\text{lept}}$ derived from measurements depending on lepton couplings only (top) and also quark couplings (bottom). Also shown is the SM prediction for $\sin^2\theta_{\text{eff}}^{\text{lept}}$ as a function of m_H . The additional uncertainty of the SM prediction is parametric and dominated by the uncertainties in $\Delta\alpha_{\text{had}}^{(5)}(m_Z^2)$ and m_t , shown as the bands. The total width of the band is the linear sum of these effects.

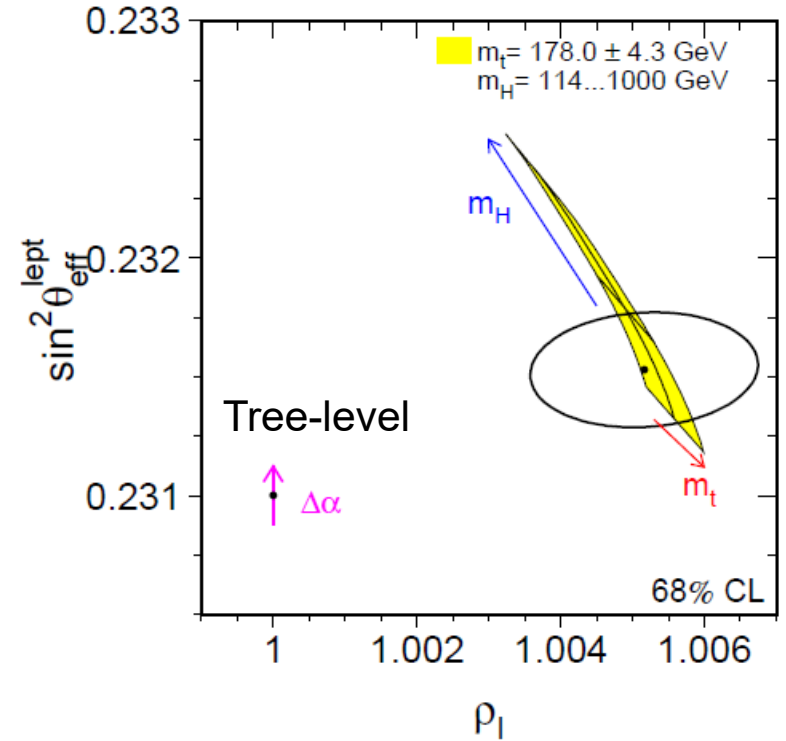
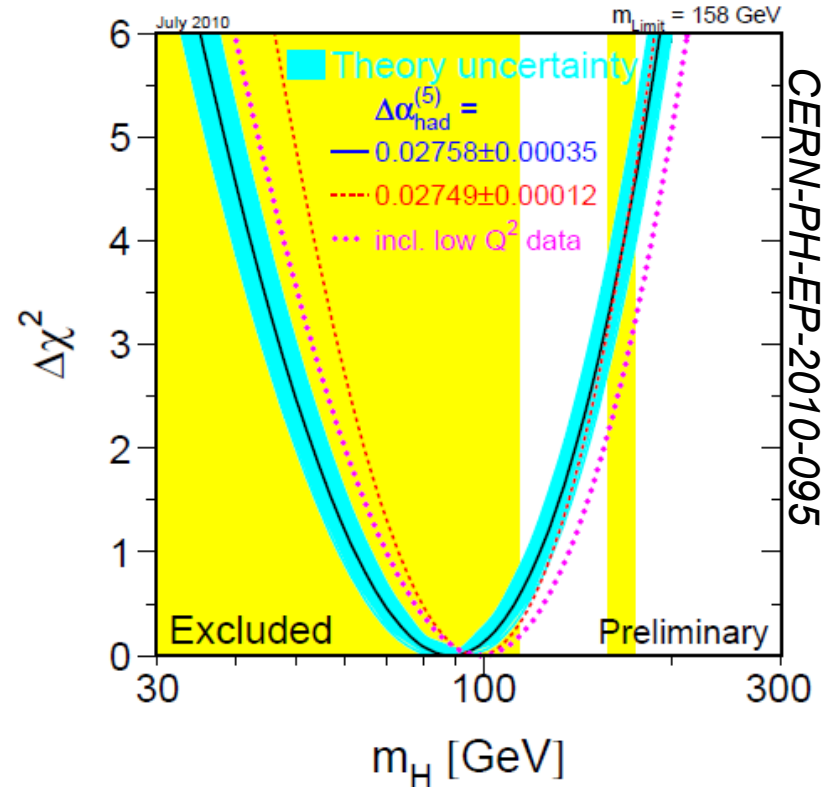
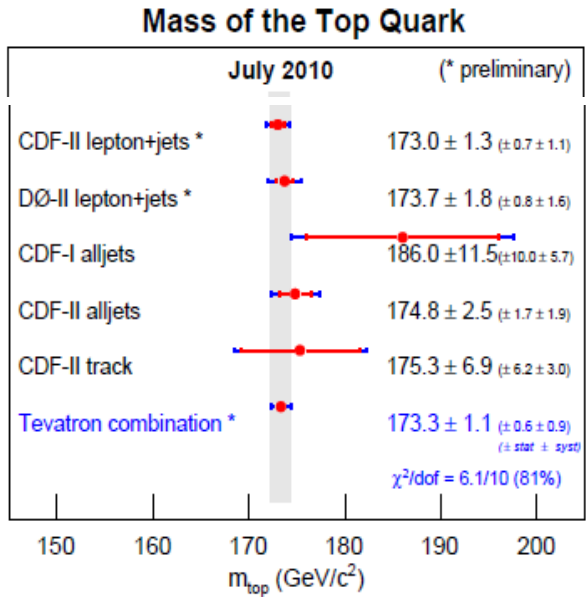


Figure 7.7: Contour curve of 68% probability in the $(\rho_l, \sin^2\theta_{\text{eff}}^{\text{lept}})$ plane. The prediction of a theory based on electroweak Born-level formulae and QED with running α is shown as the dot, with the arrow representing the uncertainty due to the hadronic vacuum polarization $\Delta\alpha_{\text{had}}^{(5)}(m_Z^2)$. The same uncertainty also affects the SM prediction, shown as the shaded region drawn for fixed $\Delta\alpha_{\text{had}}^{(5)}(m_Z^2)$ while m_t and m_H are varied in the ranges indicated.

With the discovery of the top-quark and the direct measurement of the top mass this parameter can be constrained to its experimental value and the radiative corrections allow to constrain the Higgs mass:

arXiv:1007.3178

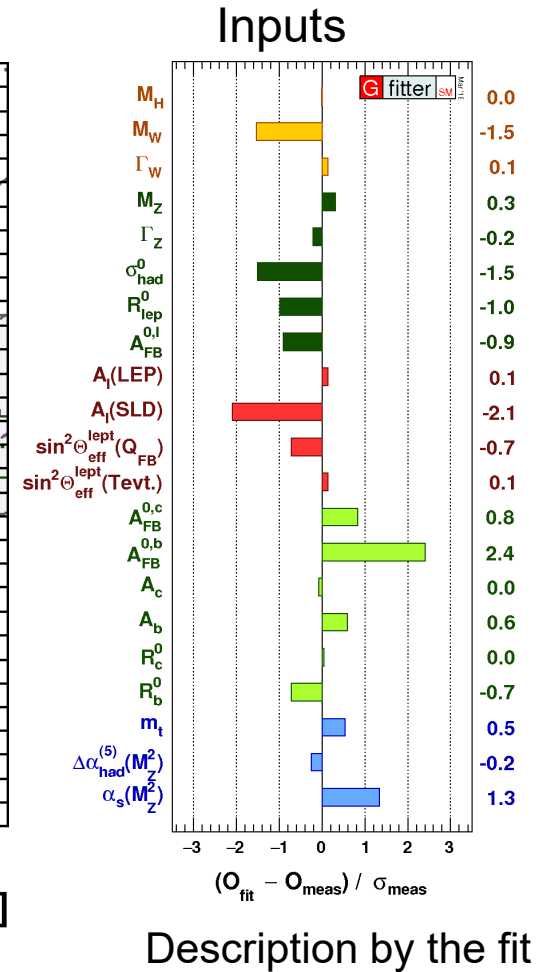
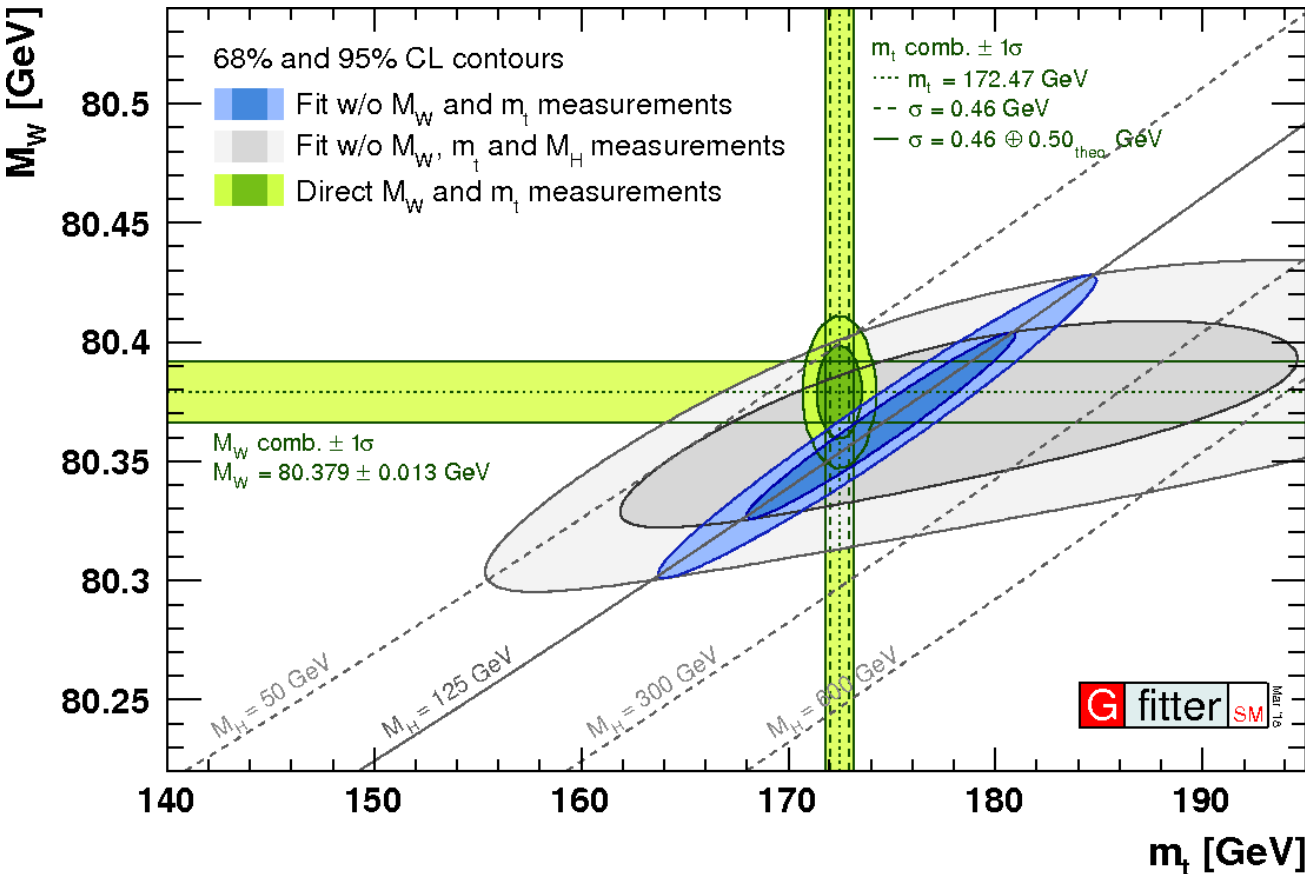


The electroweak precision data predicted a very light Higgs mass:
 Confirmed by ATLAS and CMS:
 PDG 2022: $m = 125.25 \pm 0.17 \text{ GeV}$

Figure 5: $\Delta\chi^2 = \chi^2 - \chi_{\text{min}}^2$ vs. m_H curve. The line is the result of the fit using all high- Q^2 data (last column of Table 2); the band represents an estimate of the theoretical error due to missing higher order corrections. The vertical band shows the 95% CL exclusion limit on m_H from the direct searches at LEP-II (up to 114 GeV) and the Tevatron (158 GeV to 175 GeV). The dashed curve is the result obtained using the evaluation of $\Delta\alpha_{\text{had}}^{(5)}(m_Z^2)$ from Reference 60. The dotted curve corresponds to a fit including also the low- Q^2 data from Table 3.

Test of the Predictions of Standard Model

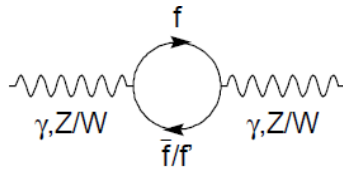
<https://project-gfitter.web.cern.ch/project-gfitter/>



Triumph of the Standard Model & success of experimental and particle physics.

Running of couplings

- Running of strong coupling α_s is well known already from PEP4
- At the Z pole we see the effect of running of α_{QED}



$$\alpha(m_Z^2) = \frac{\alpha(0)}{1 - \Delta\alpha}$$

with : $\Delta\alpha = \Delta\alpha_{\text{lept}} + \Delta\alpha_{\text{top}} + \Delta\alpha_{\text{had}}^{(5)}$

$$\alpha = \frac{1}{137} \rightarrow \alpha = \frac{1}{129}$$

- Q^2 -dependence of $\sin^2\bar{\theta}_W$

Different renormalization scheme ($\overline{\text{MS}}$ scheme).

Moller experiment at JLAB ($e^-e^- \rightarrow e^-e^-$) and P2 experiment at Mainz (MESA, $e^-p \rightarrow e^-p$): parity violating γZ interference produces LH/RH asymmetries also at very low $Q^2 \rightarrow \bar{g}_A, \bar{g}_V, \rightarrow \sin^2\bar{\theta}_W$

